

used in library construction, were harvested by the Trisolv method. NCAM, GLOBIN, XTWIST, MUSCLE ACTIN, *IFABP* (4); *Xlhxbox-8* (9); *XBRA* [P. A. Wilson and D. A. Melton, *Curr. Biol.* 4, 676 (1994)]; *EDD*, *ODC* (25); *LFABP*, up-ACCGAGATTGAACAGAATGG; down-CCTCATGTTTACCACGGAC; *MIX.1*, up-CCCAGGCATCATCAATGTC; down-TGACACGGCTCTTGGTTGGC; *MIX-ER*, up-CACAGCCAGCACTTAACC; down-CAATGTCACATCAACTGAAG; *Sox17 α* , *Sox17 β* (8).

32. In situ hybridization was performed as described in (4). Gastrula stage embryos were fixed in paraformaldehyde, cleared in butanol, and mounted in paraffin. All other sectioned material was fixed in MEMFA [0.1 M Mops (pH 7.4), 2 mM EGTA, 1 mM

Mg SO₄, 3.7% formaldehyde], cleared in xylene, and mounted in paraffin. All sections are 10 μ m thick. For *Mixer* and *Mix.1* in situ hybridization, probes were constructed from sequences 3' to the homeobox. The *Edd* and *Xbra* in situ probes have been described in [(9); J. C. Smith *et al.*, *Cell* 71, 731 (1991)]. β gal activity was measured according to standard protocols.

33. Supported in part by grants from the National Institutes of Health and the Howard Hughes Medical Institute (HHMI). G.L.H. was supported by a predoctoral grant from the National Science Foundation and D.A.M. is an investigator of the HHMI. We acknowledge the help of R. Harland for advice on expression

libraries, K. Symes for histological advice, R. Nicholls and S. Newfield for sequence alignment advice, P. Rahaim and J. Rush of the HHMI Biopolymers facility for both DNA synthesis and sequencing, E. Wu for computing advice, P. Mead for communicating data before publication, H. Woodland and D. Clements for providing *Sox17* clones, and all members of the Melton lab for helpful discussions—in particular L. Chen, Z. Balsara, S. Kim, M. Hebrok, O. Kelley, E. Wu, K. O'Donnel, C.-J. Lai, J. Wells, P. Klein, D. Kessler, and C. Dohrman.

28 October 1997; accepted 22 May 1998

Visualization of Specific B and T Lymphocyte Interactions in the Lymph Node

Paul Garside,* Elizabeth Ingulli,* Rebecca R. Merica, Julia G. Johnson, Randolph J. Noelle, Marc K. Jenkins†

Early events in the humoral immune response were visualized in lymph nodes by simultaneous tracking of antigen-specific CD4 T and B cells after immunization. The T cells were initially activated in the T cell areas when the B cells were still randomly dispersed in the B cell-rich follicles. Both populations then migrated to the edges of the follicles and interacted there, resulting in CD154-dependent B cell proliferation and germinal center formation. These results provide visual documentation of cognate T-B cell interactions and localize them to the follicular border.

Antigen-specific T and B lymphocytes are essential for humoral immune responses to many antigens (1). It is known that the T cell dependence of antibody production is related to the efficient capture and internalization of antigen by surface immunoglobulin (Ig), which allows antigen-specific B cells to efficiently present antigenic peptide-major histocompatibility complex (MHC) molecules to antigen-specific T cells (2). The T cells are thus positioned to provide stimulatory surface molecules and cytokines, thereby helping the B cells produce antibodies (3).

It is widely believed that the earliest T-B cell interactions during the primary response occur as a result of the movement of antigen-specific B cells from the B cell-rich follicles into the T cell-rich areas, where they meet antigen-specific T cells (4). However, T-B cell interactions have not been directly observed because of technical difficulties relat-

ed to simultaneous in situ detection of the rare naïve T and B cells specific for a given antigen.

We addressed this problem by tracking small populations of antigen receptor transgenic T and B lymphocytes after adoptive transfer into normal recipients. CD4 T cells from DO11.10 T cell antigen receptor (TCR) transgenic (BALB/c \times C57BL/6)F₁ mice (5) specific for chicken ovalbumin (cOVA) (amino acid residues 323 to 339) complexed to I-A^d (6) and MD4 Ig transgenic (BALB/c \times C57BL/6)F₁ mice with B cells specific for hen egg lysozyme (HEL) (7) were transferred (8) into nontransgenic (BALB/c-Igh^b \times C57BL/6)F₁ animals. The DO11.10 CD4 T cells were identified in the lymph nodes of the recipients by flow cytometry after staining with the anti-clonotypic TCR monoclonal antibody (mAb) KJ1-26 (9); labeled HEL or antibody specific for the IgM^a (anti-HEL Ig) allotype was used to identify MD4 B cells (10).

cOVA was chemically coupled to HEL to produce an antigen (cOVA-HEL) containing linked epitopes that could be recognized by both transgenic populations (cOVA-HEL) (11). Immunization with cOVA-HEL caused the DO11.10 CD4 T cells in the draining lymph nodes to undergo clonal expansion that was apparent by day 2, was maximal on days 3 and 4, and declined thereafter (Fig. 1A).

MD4 B cell expansion in the lymph nodes was detected 3 days after immunization, peaked on day 4 or 5, and then declined (Fig. 1A). Maximal clonal expansion of the DO11.10 T cells, because a much reduced response was observed in mice that received B cells alone (Fig. 1A). The MD4 B cells responded weakly when recipients of DO11.10 T cells and MD4 B cells were immunized with a mixture of cOVA and HEL that had been conjugated to turkey OVA (tOVA-HEL) (Fig. 1B), which lacks the appropriate peptide recognized by the DO11.10 TCR (Fig. 1C). The poor response of the B cells in this situation could not be explained by a failure of T cell activation because the DO11.10 T cells responded well after immunization with cOVA plus tOVA-HEL (Fig. 1C). The simplest explanation for these results is that MD4 B cells were efficiently activated to proliferate in vivo only when expression of anti-HEL Ig allowed efficient uptake of cOVA and presentation of cOVA peptide to DO11.10 T cells.

This conclusion was supported by the finding that blockage of CD154 (CD40 ligand), a surface molecule expressed by activated CD4 T cells that provides a contact-dependent signal to B cells (12), completely inhibited clonal expansion (Fig. 1D) and antibody production (13) by the MD4 B cells. In contrast, treatment with antibody to CD154 (anti-CD154) inhibited clonal expansion of the DO11.10 T cells by only about 50% (Fig. 1D). These findings suggest that the previously described effects of CD154 blockade on antibody production and germinal center formation (12) can be explained by a failure of B cell clonal expansion.

Immunohistochemical analyses were carried out to determine whether the cognate interactions predicted by the functional experiments could be directly observed in situ. After adoptive transfer, but before immunization, the DO11.10 T cells were dispersed throughout the T cell-rich paracortical regions of the lymph node but were not present in the B cell-rich follicles (Fig. 2A). In contrast, the MD4 B cells were localized mainly in follicles (Fig. 2E). One day after immunization, the DO11.10 T cells had not increased

P. Garside, University of Glasgow, Department of Immunology, Western Infirmary, Glasgow, G11 6NT, United Kingdom. E. Ingulli, Department of Pediatrics, University of Minnesota Medical School, Minneapolis, MN 55455, USA. R. R. Merica, J. G. Johnson, M. K. Jenkins, Department of Microbiology and the Center for Immunology at the University of Minnesota Medical School, Minneapolis, MN 55455, USA. R. J. Noelle, Dartmouth Medical College, Department of Microbiology, Lebanon, NH, USA.

*These authors contributed equally to this work.

†To whom correspondence should be addressed.

REPORTS

in number but were present in small clusters within the paracortex (Fig. 2B). At this time, the MD4 B cells were difficult to detect at the magnification shown (Fig. 2F). However, inspection at a higher magnification revealed that MD4 B cells were still randomly distributed in the follicles, although the intensity of anti-IgM^a staining on the MD4 B cells was greatly reduced (compare Fig. 2, E and F insets).

Two days after immunization, the DO11.10 T cells began to increase in number in the paracortex and, as described in (14, 15), moved into the edges of the follicles (Figs. 2C and 3A). IgM^a was again easily detected on the MD4 B cells, which had increased slightly in number, and redistributed to the edges of the follicles (Figs. 2G and 3B) where

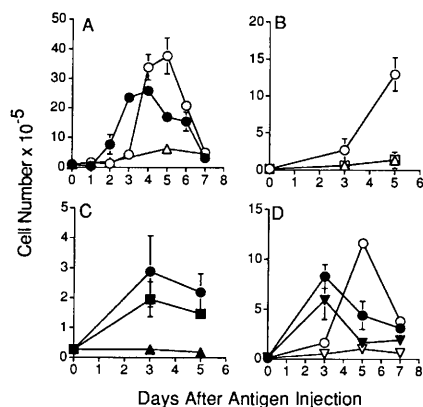


Fig. 1. Kinetics of CD4 T and B cell clonal expansion. (A) (BALB/c-Igh^b × C57BL/6)_F₁ recipients of DO11.10 T cells and MD4 B cells or MD4 B cells alone were injected with cOVA-HEL (17). The mean number ± SD of CD4⁺ DO11.10 T cells (closed circles) or IgM^a MD4 B cells (open circles) in recipients of DO11.10 T cells and MD4 B cells or IgM^a MD4 B cells (triangles) in recipients of MD4 B cells alone was measured in the draining lymph nodes at the indicated time points by multiplying the number of viable cells in the lymph nodes by the percentage of DO11.10 T or MD4 B cells present as assessed by flow cytometry (8). (B and C) (BALB/c-Igh^b × C57BL/6)_F₁ recipients of DO11.10 T cells and MD4 B cells were injected subcutaneously with CFA containing 130 μg of cOVA-HEL (circles), 130 μg of tOVA-HEL (triangles), or 100 μg of cOVA plus 130 μg of tOVA-HEL (squares). The mean number ± SD of MD4 B cells (B) or DO11.10 T cells (C) present in draining lymph nodes was measured at the indicated time points after injection of antigen. (D) (BALB/c-Igh^b × C57BL/6)_F₁ recipients of DO11.10 T cells and MD4 B cells were injected with cOVA-HEL (17) on day 0 and intraperitoneally with 250 μg of anti-CD154 mAb (clone MR1) or control hamster Ig on days 0, 2, and 4. The mean number of cells ± SD in mice injected with cOVA-HEL and control Ig (DO11.10, closed circles; MD4, open circles) or with cOVA-HEL and anti-CD154 mAb (DO11.10, closed inverted triangles; MD4, open inverted triangles) are shown for the indicated time points.

the DO11.10 T cells were located (Fig. 3C). About 70% of the DO11.10 T cells were in physical contact with one or more MD4 B cells (Fig. 3D) in the rim of the follicles after injection of cOVA-HEL. The specificity of these interactions was indicated by the find-

ing that only about 10% of the DO11.10 T cells located in the follicular rim were found in physical contact with MD4 B cells after injection of cOVA plus tOVA-HEL (Fig. 3E), a situation in which cognate interactions would not be expected. Few, if any, interac-

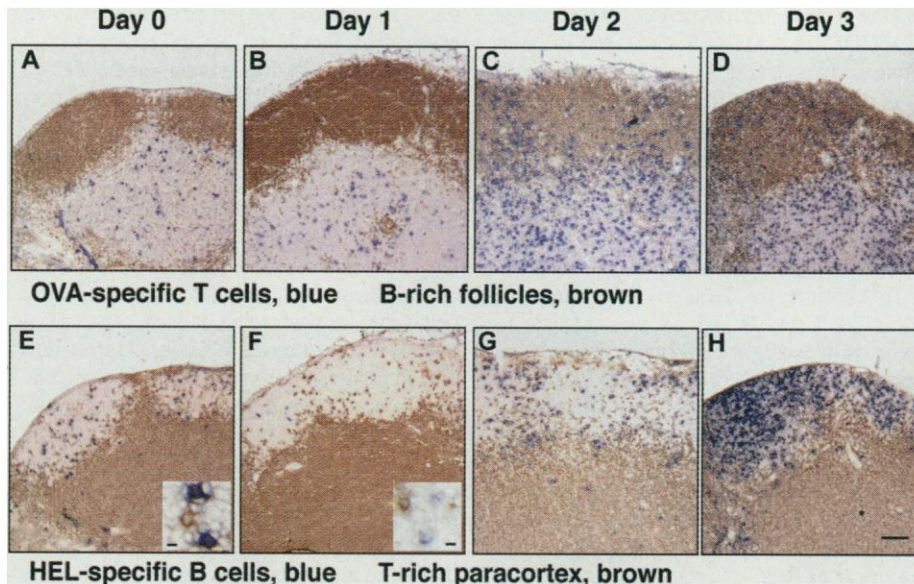
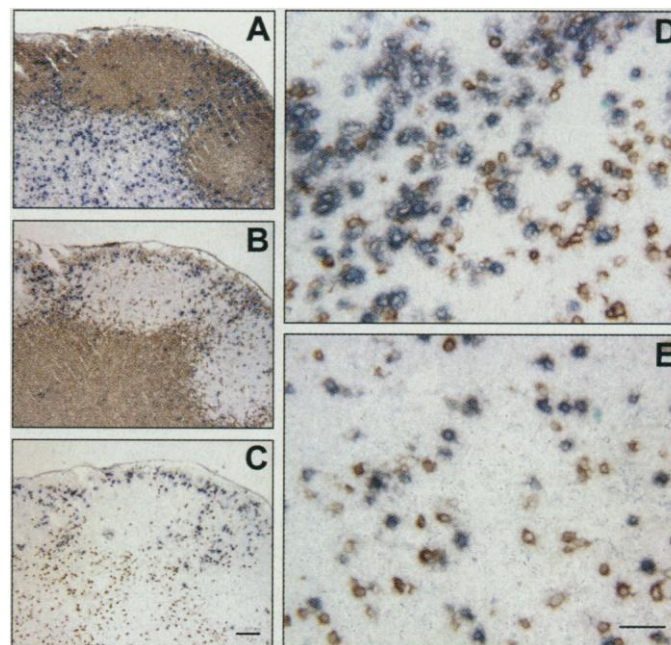


Fig. 2. Anatomic localization of DO11.10 T cells and MD4 B cells during the primary response. (BALB/c-Igh^b × C57BL/6)_F₁ recipients of DO11.10 T cells and MD4 B cells were injected with cOVA-HEL (17). Mice were sacrificed 0 (A and E), 1 (B and F), 2 (C and G), or 3 (D and H) days after immunization and the draining lymph nodes were sectioned and stained (27). (A) and (E), (B) and (F), (C) and (G), and (D) and (H) were from adjacent sections. (A to D) KJ1-26⁺ DO11.10 T cells are stained blue, and B220⁺ B cells are stained brown to identify the follicles. (E to H) IgM^a MD4 B cells are stained blue, and Thy 1.2⁺ T cells are stained brown to identify the T cell-rich paracortical areas. Bar = 50 μm. (Insets) High-power views of areas within the follicles of (E) and (F). Inset scale bars = 5 μm.

Fig. 3. Colocalization of DO11.10 T cells and MD4 B cells at the follicular border 2 days into the primary response. (BALB/c-Igh^b × C57BL/6)_F₁ recipients of DO11.10 T cells and MD4 B cells were injected with cOVA-HEL (17). The draining lymph nodes were harvested on day 2, sectioned, and stained (27). (A) B220⁺ B cells are stained brown and KJ1-26⁺ DO11.10 T cells are stained blue. (B) Thy 1.2⁺ T cells are stained brown and IgM^a MD4 B cells are stained blue. (C) KJ1-26⁺ DO11.10 T cells are stained brown and IgM^a MD4 B cells are stained blue. (A) to (C) are from adjacent areas of the same lymph node. Bar = 50 μm. Higher-power views of the edges of lymph node follicles 2 days after subcutaneous injection of CFA containing 130 μg of cOVA-HEL (D) or 100 μg of cOVA plus 130 μg of tOVA-HEL (E) are shown. KJ1-26⁺ DO11.10 T cells are stained brown and IgM^a MD4 B cells are stained blue. Scale bar = 25 μm.



REPORTS

tions between DO11.10 T cells and MD4 B cells were observed in the T cell-rich paracortex at this time (Fig. 3C) or at any time (Fig. 2) after injection of cOVA-HEL.

Over the next 2 days after immunization with cOVA-HEL, the DO11.10 T cells continued to accumulate in the paracortex and became evenly distributed in the follicles (Fig. 2D). The MD4 B cells proliferated between days 2 and 3 and were present in small clusters in the follicles on day 3 (Fig. 2H) and in peanut agglutinin-positive germinal centers on day 4 (Fig. 4). Large, darkly staining IgM⁺ MD4 B cells, presumably plasma cells (16), accumulated within the medulla when germinal centers appeared (Fig. 4A, arrow).

By elevating the frequency of antigen-specific CD4 T and B cells, it was possible to define early events in the primary immune response. We found T cells in small clusters in the T cell areas as early as 1 day after immunization. In previous studies, these clusters were found to result from interactions between T cells and dendritic cells of the recipient (16, 17). At this time, the B cells were still randomly distributed throughout the follicles but had lost much of their Ig, probably as a result of

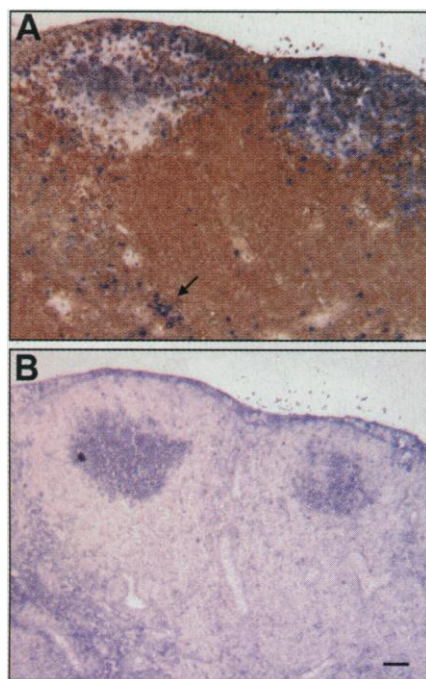


Fig. 4. Germinal center formation and the appearance of B cells in the medulla 4 days into the primary response. (BALB/c-Igh^b × C57BL/6)F₁ recipients of DO11.10 T cells and MD4 B cells were injected with cOVA-HEL (11). The draining lymph nodes were harvested on day 4, sectioned, and stained (27). (A) Thy 1.2⁺ T cells are stained blue, and IgM⁺ MD4 B cells are stained brown. MD4 B cells expressing high levels of IgM⁺ and present in the medulla are indicated with an arrow. (B) Peanut agglutinin-positive cells are stained blue. Scale bar = 50 μm.

internalization and degradation of surface Ig-HEL complexes (18). The lack of physical interactions between antigen-specific T and B cells at this time is evidence that T cell interactions with dendritic cells precede those with B cells even in a situation in which the number of antigen-specific B cells is unlikely to be limiting. This ordered antigen presentation would ensure that T cells are always activated by a dendritic cell first, thus avoiding initial antigen presentation by B cells, which has been shown to delete or inactivate naïve T cells (19).

Elevation of the frequency of antigen-specific cells also allowed identification of cognate T-B cell interactions and localized them to the edge of the B cell-rich follicles 2 days after immunization. The interactions occurred there because both antigen-specific cell types moved toward each other from their separate starting locations. Our studies extend previous findings that antigen-specific B cells in the spleen accumulate at the border between the follicles and the T cell areas in the presence of antigen (20, 21) by showing that antigen-specific helper T cells are physically interacting with the B cells in this location. Furthermore, our results show that cognate interactions in the lymph node initially take place on the B cell side of this border and not on the T cell side as has been widely believed (4). Our results also shed light on the relevance of the foci of antigen-specific B cells that form in the T cell areas of the spleen in response to some antigens (20) and have been suggested to be the source of germinal center B cells (22). Foci were not observed in the T cell areas of the lymph nodes in our studies; all the initial B cell clonal expansion and subsequent germinal center formation occurred in the follicles. Thus, our study and another (23) indicate that T-B cell interactions in extrafollicular foci are not necessary for antibody production and germinal center formation.

The results presented here suggest a model in which antigen-specific B cells move to the edge of the follicles shortly after immunization and present peptide-MHC complexes to specific CD4 T cells that have recently entered this site after activation by dendritic cells. The B cells then receive lymphokines and CD154 signals from the T cells and proliferate in the follicles. Some of these B cells remain in the follicles and become membrane Ig-expressing germinal center cells. Others become antibody-secreting plasma cells and move to the medulla, probably on their way to the bone marrow (24).

References and Notes

1. N. A. Mitchison, *Eur. J. Immunol.* **1**, 18 (1971); M. C. Raff, *Nature* **226**, 1257 (1970); E. S. Vitetta, B. R. Fernandez, C. D. Myers, V. M. Sanders, *Adv. Immunol.* **45**, 1 (1989).

2. A. Lanzavecchia, *Nature* **314**, 537 (1985).
3. H. Kupfer, C. R. Monks, A. Kupfer, *J. Exp. Med.* **179**, 1507 (1994); E. A. Clark and J. A. Ledbetter, *Nature* **367**, 425 (1994).
4. G. Kelsoe, *Immunity* **4**, 107 (1996); I. C. MacLennan *et al.*, *Immunol. Rev.* **156**, 53 (1997).
5. The DO11.10 TCR has been reported to possess a weak alloreactivity for the I-A^b molecule expressed in C57BL/6 mice (25), raising the possibility that the DO11.10 T cells would be deleted during development in (BALB/c × C57BL/6)F₁ mice (26). Indeed, DO11.10 (BALB/c × C57BL/6)F₁ mice consistently yielded a lower number of CD4⁺ KJ1-26⁺ lymph node T cells than their BALB/c counterparts, probably as a consequence of a certain degree of thymic deletion. The peripheral KJ1-26⁺ cells in DO11.10 (BALB/c × C57BL/6)F₁ mice also contained more CD4⁺ CD8⁻ T cells than DO11.10 BALB/c mice. However, most CD4⁺ KJ1-26⁺ cells in DO11.10 (BALB/c × C57BL/6)F₁ mice possessed the surface phenotype of naïve T cells (CD45RB^{high}) and were clearly capable of undergoing extensive clonal expansion *in vivo* after adoptive transfer and immunization (Fig. 1).
6. K. M. Murphy, A. B. Heimberger, D. Y. Loh, *Science* **250**, 1720 (1990).
7. C. C. Goodnow *et al.*, *Nature* **334**, 676 (1988).
8. Before adoptive transfer, spleen and lymph node cells from DO11.10 (BALB/c × C57BL/6)F₁ donor mice were depleted of CD8 T and B cells and a sample was stained with phycoerythrin (PE)-labeled anti-CD4 mAb (Pharmingen) and biotinylated KJ1-26 mAb followed by fluorescein isothiocyanate (FITC)-labeled streptavidin (Caltag) as described in (74). Similarly, a sample of spleen and lymph node cells from MD4 (BALB/c × C57BL/6)F₁ mice was stained with PE-labeled anti-B220 mAb (Pharmingen) in combination with biotinylated HEL or biotinylated anti-IgM^a mAb (Pharmingen) followed by FITC-labeled streptavidin. Stained cells (20,000 events per sample) were then analyzed on a flow cytometer and the percentages of DO11.10 CD4 T cells and MD4 B cells were determined. Cell suspensions containing 1 to 2.5 × 10⁶ DO11.10 CD4 T cells and 2.5 to 5 × 10⁶ MD4 B cells were then injected intravenously into (BALB/c-Igh^b × C57BL/6)F₁ recipients.
9. K. Haskins *et al.*, *J. Exp. Med.* **157**, 1149 (1983).
10. In a representative flow cytometry experiment, CD4⁺ KJ1-26⁺ DO11.10 T cells accounted for 0.5% of viable lymph node cells before immunization of (BALB/c-Igh^b × C57BL/6)F₁ recipients of DO11.10 T cells and MD4 B cells. This percentage increased to 4.1% 5 days after immunization with cOVA-HEL (71). We detected no CD4⁺ KJ1-26⁺ events in untransferred (BALB/c-Igh^b × C57BL/6)F₁ before or after immunization, which indicates that only transferred cells were detected. B220⁺ HEL-binding or IgM^a MD4 B cells accounted for 0.5 or 1.5% of viable lymph node cells, respectively, before recipients of both transgenic populations were immunized. The disparity between these values is related to the fact that the anti-IgM^a mAb detects slightly more background events in untransferred recipients (0.18%) than does HEL (0.06%). In addition, a small percentage (about 10%) of B cells in the MD4 transgenic mice express IgM^a but do not bind HEL, probably because of expression of an endogenous light chain. The percentages of B220⁺ HEL-binding and IgM^a MD4 B cells increased to 8.0 and 8.8%, respectively, 5 days after immunization with cOVA-HEL (71).
11. We prepared cOVA-HEL by using glutaraldehyde to couple HEL (Biozyme Laboratories) to cOVA (Sigma). One hundred and thirty micrograms of cOVA-HEL was estimated to contain the equivalent of 100 μg of cOVA and 30 μg of HEL. We injected mice subcutaneously on the back with 130 μg of cOVA-HEL in complete Freund's adjuvant (CFA) and harvested the draining cervical, axillary, and brachial lymph nodes at various times after the immunization. We determined the percentage of CD4⁺ KJ1-26⁺ DO11.10 T cells and B220⁺ IgM^a MD4 B cells as described in (8).
12. T. M. Foy, A. Aruffo, J. Bajorath, J. E. Buhlmann, R. J. Noelle, *Annu. Rev. Immunol.* **14**, 591 (1996).
13. P. Garside, unpublished data.
14. E. R. Kearney, K. A. Pape, D. Y. Loh, M. K. Jenkins, *Immunity* **1**, 327 (1994).

15. B. Zheng, S. Han, G. Kelsoe, *J. Exp. Med.* **184**, 1083 (1996); K. A. Fuller, O. Kanagawa, M. H. Nahm, *J. Immunol.* **151**, 4505 (1993); A. Gulbranson-Judge and I. MacLennan, *Eur. J. Immunol.* **26**, 1830 (1996).
16. S. A. Luther, A. Gulbranson-Judge, H. Acha-Orbea, I. C. M. MacLennan, *J. Exp. Med.* **185**, 551 (1997).
17. E. Ingulli, A. Mondino, A. Khoruts, M. K. Jenkins, *ibid.*, p. 2133.
18. J. Braun, P. S. Hochman, E. R. Unanue, *J. Immunol.* **128**, 1198 (1982).
19. E. E. Eynon and D. C. Parker, *J. Exp. Med.* **175**, 131 (1992); E. J. Fuchs and P. Matzinger, *Science* **258**, 1156 (1992).
20. J. Jacob, R. Kassir, G. Kelsoe, *J. Exp. Med.* **173**, 1165 (1991).
21. W. J. Liu, J. Zhang, P. J. L. Lane, E. Y. T. Chan, I. C. M. MacLennan, *Eur. J. Immunol.* **21**, 2951 (1991); J. C. Cyster and C. C. Goodnow, *Immunity* **3**, 691 (1995).
22. J. Jacob and G. Kelsoe, *J. Exp. Med.* **176**, 679 (1992).
23. K. A. Vora, K. M. Tumas-Brundage, T. Manser, *J. Immunol.* **160**, 728 (1998).
24. M. K. Slifka, R. Antia, J. K. Whitmire, R. Ahmed, *Immunity* **8**, 363 (1998).
25. R. Shimonkevitz, J. Kappler, P. Marrack, H. Grey, *J. Exp. Med.* **158**, 303 (1983).
26. C. P. Liu, J. W. Kappler, P. Marrack, *ibid.* **184**, 1619 (1996).
27. Draining lymph nodes were harvested and frozen in liquid nitrogen in O.C.T. embedding medium (Miles). Tissue sections (10 μ m) were cut on a Cryostat microtome, fixed in acetone, and blocked with goat serum. Sections were stained sequentially with biotinylated KJ1-26, anti-IgM⁺, or peanut agglutinin; avidin-biotin complex-labeled alkaline phosphatase; and 5-bromo-4-chloro-3-indolyl phosphate/nitroblue tetrazolium substrate, followed by biotinylated anti-B220, anti-Thy 1.2, or KJ1-26; avidin-biotin complex-labeled peroxidase; and 3,3'-diaminobenzidine sub-

strate (Vector). Development of the first avidin-biotin complex-labeled enzyme destroyed residual avidin binding sites on the primary antibodies, thereby preventing artifactual binding of the second avidin-biotin complex-labeled enzyme. The weak background anti-IgM⁺ staining mentioned in (10) was not detected on tissue sections and thus has no bearing on the immunohistology experiments.

28. We thank J. Walter and M. Michels for technical assistance and T. Behrens, D. Mueller, M. Mescher, J. Cyster, and K. Hogquist for helpful discussions. Supported by grants from NIH (AI27998, AI35296, and AI39614 to M.K.J.; K08-AI01503 and HD33692 to E.L.; and AI07421 to R.R.M.), the University Children's Foundation (E.L.), the Vikings Children's Fund (E.L.), and the Wellcome Trust (P.G.).

26 March 1998; accepted 26 May 1998

C₁ Transfer Enzymes and Coenzymes Linking Methylo-trophic Bacteria and Methanogenic Archaea

Ludmila Chistoserdova, Julia A. Vorholt, Rudolf K. Thauer, Mary E. Lidstrom*

Methanogenic and sulfate-reducing Archaea are considered to have an energy metabolism involving C₁ transfer coenzymes and enzymes unique for this group of strictly anaerobic microorganisms. An aerobic methylo-trophic bacterium, *Methylobacterium extorquens* AM1, was found to contain a cluster of genes that are predicted to encode some of these enzymes and was shown to contain two of the enzyme activities and one of the methanogenic coenzymes. Insertion mutants were all unable to grow on C₁ compounds, suggesting that the archaeal enzymes function in aerobic C₁ metabolism. Thus, methylo-trophy and methanogenesis involve common genes that cross the bacterial/archaeal boundaries.

Methylobacterium strains are obligately aerobic bacteria capable of growing on one-carbon (C₁) compounds (methylo-trophs) (1). They contain a well-known pathway for interconverting C₁ compounds that involves a folate coenzyme, tetrahydrofolate (H₄F), and nicotinamide adenine dinucleotide phosphate [NAD(P)] (Fig. 1A) (1–3). It has been postulated that in *Methylobacterium* strains this pathway operates in the oxidative direction to convert formaldehyde to CO₂, generating reduced pyridine nucleotides and serving as a major energy-generating pathway during growth on C₁ compounds (2, 3). The strictly anaerobic

Archaea that produce methane (methanogens) or that grow on acetate by sulfate reduction (*Archaeoglobus*) carry out analogous reactions that use a different coenzyme, tetrahydromethanopterin (H₄MPT), and a furan-type cofactor, methanofuran (MFR), and involve either H₂ or the electron acceptor/donor F₄₂₀ rather than NAD(P) (Fig. 1B). In the methanogenic Archaea, these reactions are part of the pathway that reduces CO₂ to methane, the central pathway for energy metabolism in methanogens (4). In the sulfate-reducing archaeon *Archaeoglobus*, the H₄MPT- and MFR-linked reactions shown in Fig. 1B operate in the oxidative direction, as part of the energy metabolism for utilizing acetate (5). Thus, the H₄MPT/MFR-linked enzymes have until now only been found in methanogenic and sulfate-reducing Archaea, whereas the H₄F-linked enzymes have been found in Bacteria, Eukarya, and some Archaea. This separation has suggested that the two sets of pathways are evolutionarily distinct, with the H₄MPT/MFR-linked pathways arising after the sep-

aration of the methanogenic and sulfate-reducing Archaea from other evolutionary branches.

One of the aerobic methylo-trophs that has been well studied is the α -proteobacterium *Methylobacterium extorquens* AM1. This bacterium contains nine clusters of genes involved in growth on C₁ compounds (6). The largest of these is ~30 kb and contains the gene for NADP-dependent methylene H₄F dehydrogenase (*mtdA*) as well as a number of other methylo-trophy genes (6). We recently cloned and sequenced a 14-kb region adjacent to one end of this 30-kb gene cluster (7) and found that it contains 13 new open reading frames (Fig. 2). The translated products of 12 of these are similar to those of genes in methanogens (8) or in *Archaeoglobus fulgidus* (9), or both, but not to any other entries in the databases, whereas the amino acid sequence translated from one (*orfX*) is similar to the sequence of *M. extorquens* AM1 MtdA but not to any archaeal polypeptide entries (percent identical amino acids is shown in Table 1). The products of six of these methanogen-like genes (*orfY*, *orf4*, *orf7*, *orf9*, *orf17*, and *orf18*) are similar to unidentified gene products in archaeal genome sequences. The other six are similar to the translated products for known genes of the H₄MPT/MFR pathway in methanogens and *A. fulgidus*, and to another archaeal protein (Fig. 1B and Table 1): FfsA is similar to formyl MFR:H₄MPT formyltransferase; OrfZ to methenyl H₄MPT cyclohydro-lase; Orf1, Orf2, and Orf3 to three of the six subunits for formyl MFR dehydrogenase, including the catalytic (B) subunit (10); and Orf5 to ribosomal protein S6 modification protein (a methylase) in *Methanococcus jannaschii* (8). Alignments of the putative methenyl H₄MPT cyclohydro-lase and formyl MFR:H₄MPT formyltransferase sequences with known sequences in the database reveal strong conservation of groups of amino acid residues between all of the sequences (Fig. 3) (11).

L. Chistoserdova, Department of Chemical Engineering, University of Washington, Seattle, WA 98195, USA. J. A. Vorholt and R. K. Thauer, Department of Biochemistry, Max-Planck-Institute for Terrestrial Microbiology, Marburg 35043, Germany. M. E. Lidstrom, Department of Chemical Engineering, Department of Microbiology, University of Washington, Seattle, WA 98195, USA.

*To whom correspondence should be addressed. E-mail: lidstrom@u.washington.edu